Cell Reports

Supplemental Information

Histone H3 Serine 28 Is Essential for Efficient Polycomb-Mediated Gene Repression in *Drosophila*

Philip Yuk Kwong Yung, Alexandra Stuetzer, Wolfgang Fischle, Anne-Marie Martinez, and Giacomo Cavalli

Supplemental Information

Supplemental Figures S1-S4

- **Figure S1, Related to Figure 1. Schematic overview of the system for assaying the function of H3S28 and validation on histone replacement clones in larval imaginal discs.**
- **Figure S2, related to Figure 2. Hox gene derepression profiles in histone mutants (*H3S28A* and *H3K27R*) clones and *Antp*^{Ns}.**
- **Figure S3, related to Figure 3. Validation of clone induction of *dUtxΔ, H3S28A* double mutant and of in vivo RNAi against Aurora B kinase.**
- **Figure S4, related to Figure 2. Nuclear staining patterns of Ph remain unchanged in *H3S28A* mutant.**

Supplemental Figure Legends S1-S4

Supplemental Experimental Procedures

Supplemental References

Supplemental Figures
Figure S1

A

```
S. pombe          ARTKQTARKSTGGKAPRKQLASKAARKAAPATGGVKKPHRYRPGTVALRE
T. thermophila    ARTKQTARKSTGAKAPRKQLASKAARKSAPATGGIKKPHRFRPGTVALRE
N. crassa         ARTKQTARKSTGGKAPRKQLASKAARKSAPSTGGVKKPHRYKPGTVALRE
D. melanogaster   ARTKQTARKSTGGKAPRKQLATKAARKSAPATGGVKKPHRYRPGTVALRE
X. laevis         ARTKQTARKSTGGKAPRKQLATKAARKSAPATGGVKKPHRYRPGTVALRE
D. rerio          ARTKQTARKSTGGKAPRKQLATKAARKSAPATGGVKKPHRYRPGTVALRE
M. musculus       ARTKQTARKSTGGKAPRKQLATKAARKSAPATGGVKKPHRYRPGTVALRE
H. sapiens        ARTKQTARKSTGGKAPRKQLATKAARKSAPATGGVKKPHRYRPGTVALRE
A. thaliana       ARTKQTARKSTGGKAPRKQLATKAARKSAPATGGVKKPHRFRPGTVALRE
                  1                         27
```

B

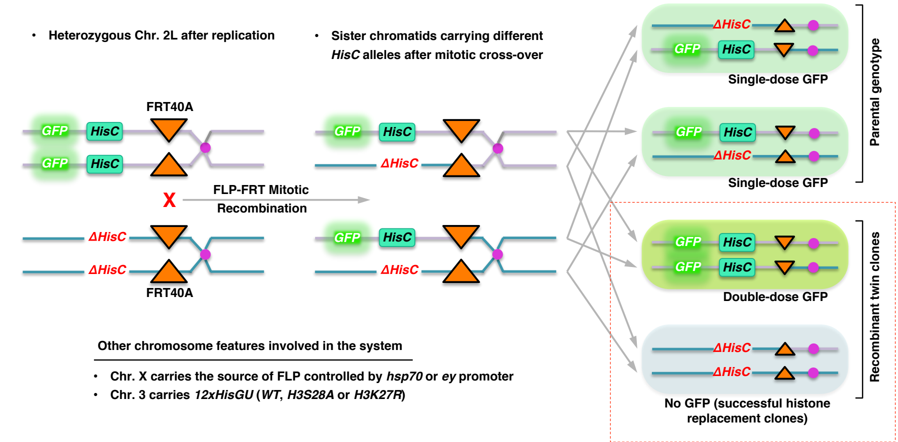

C

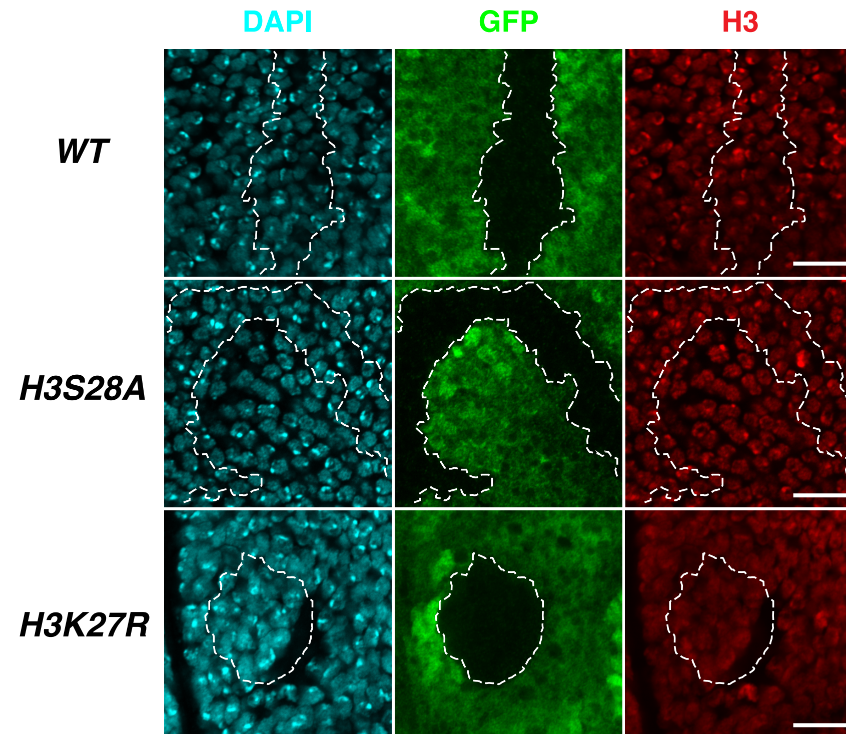

D

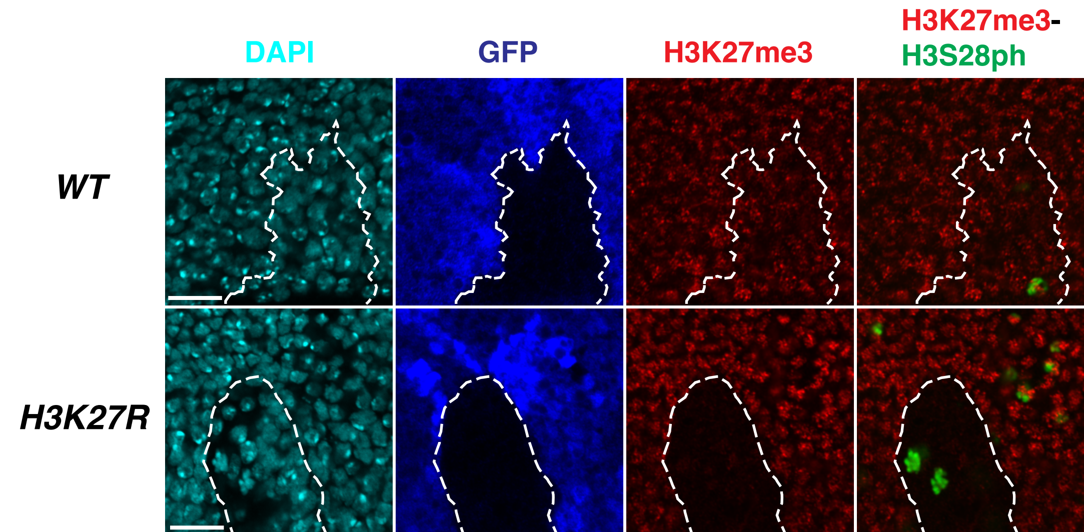

Figure S2

A

GFP+Scr: eye-antenna, 2nd leg, 3rd leg, wing

GFP+Antp: eye-antenna

GFP+Abd-B: eye-antenna, wing

GFP+Ubx: eye-antenna, wing

WT

H3S28A

H3K27R

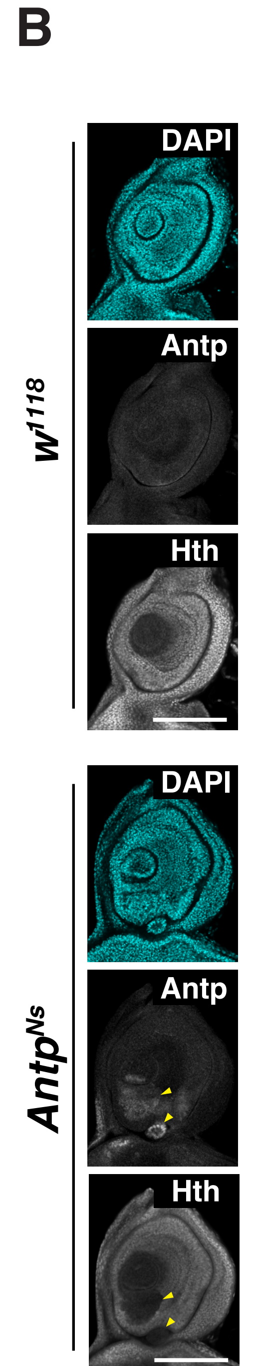

Figure S3

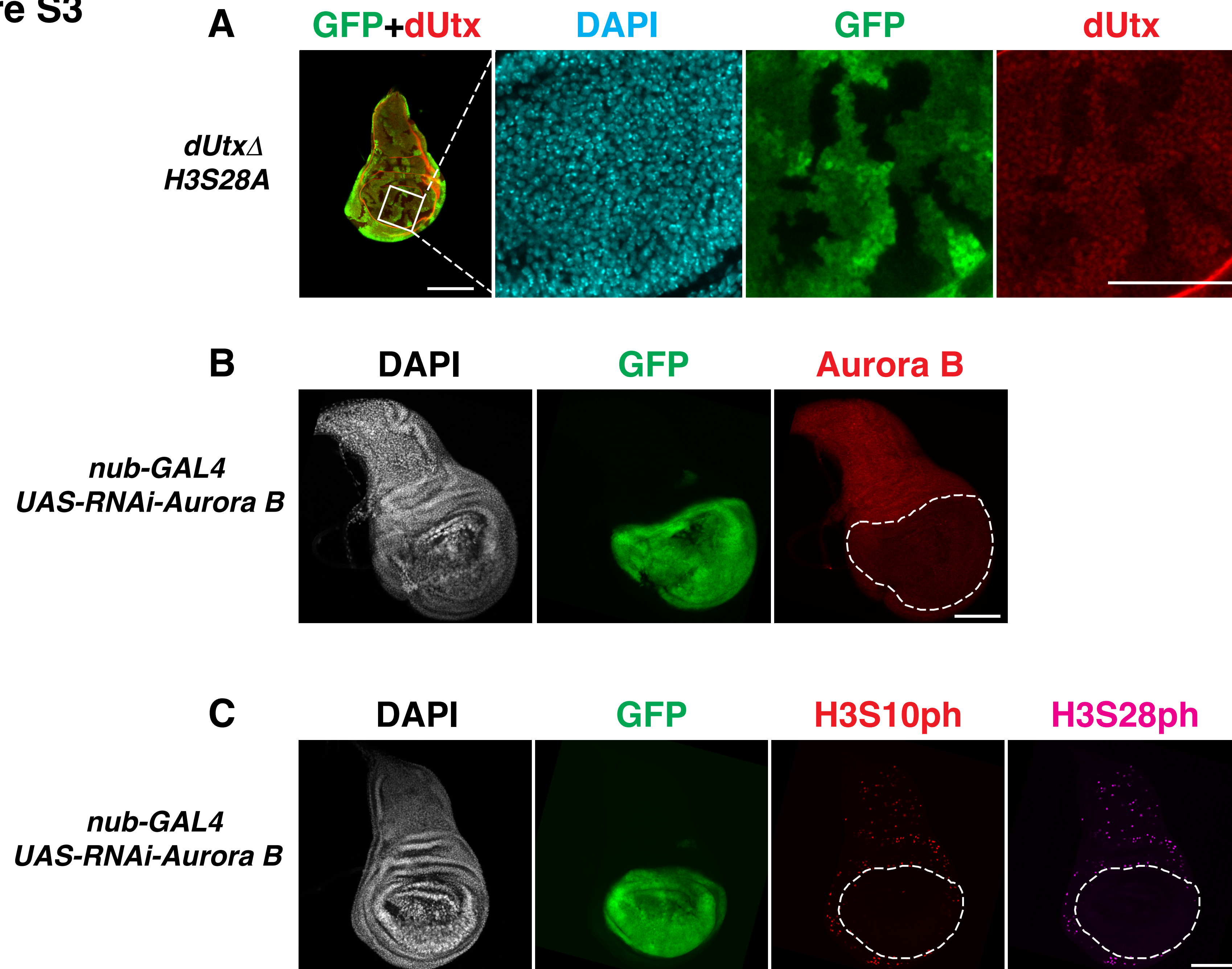

Figure S4

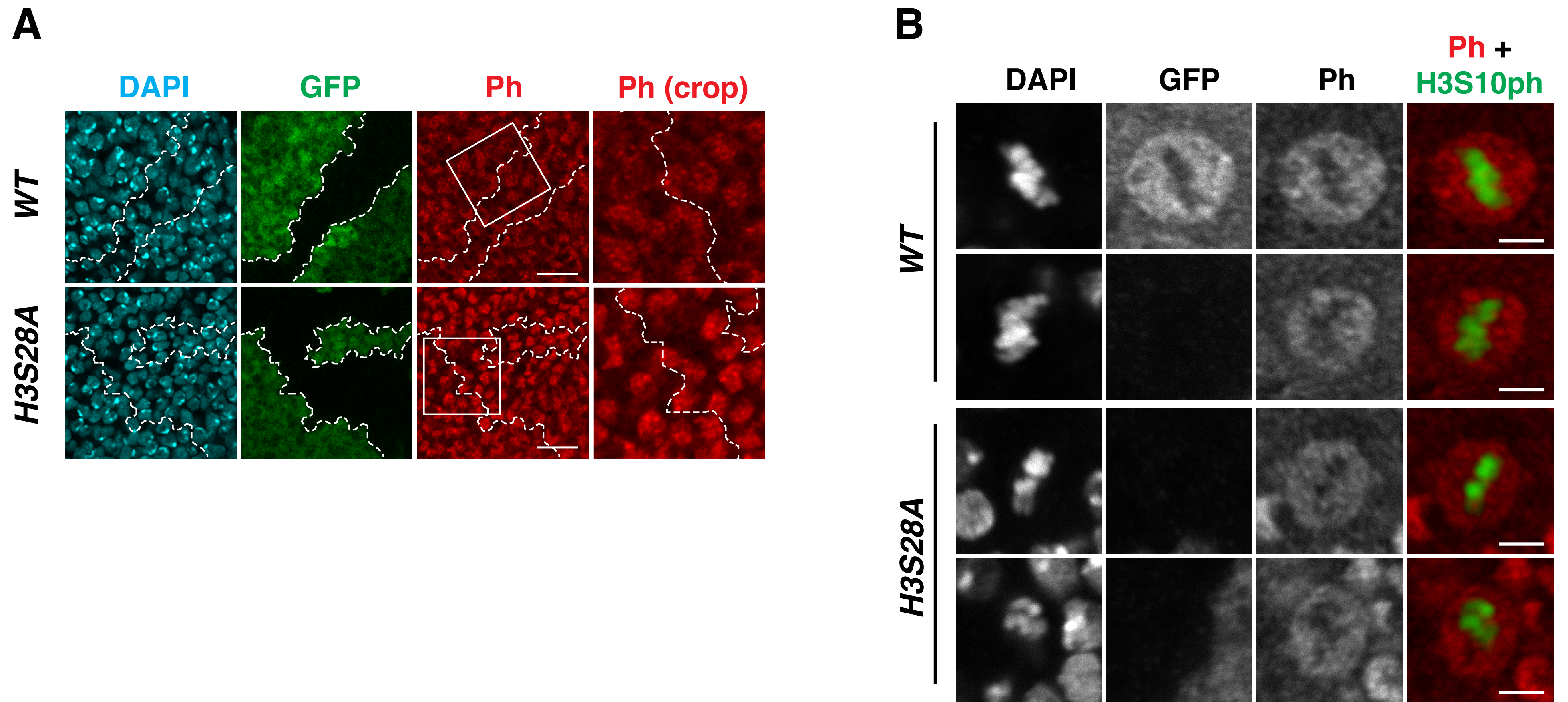

Supplemental Figure Legends

Figure S1, Related to Figure 1. Schematic overview of the system for assaying the function of H3S28 and validation on histone replacement clones in larval imaginal discs.

(A) The serine residue at position 28 of the histone H3 protein is conserved. Alignment of the N-terminal 1-50 amino acids of H3 from various eukaryotes. H3K27, the methylation target site of PRC2, is highlighted in red; the conserved H3S28 residue is highlighted in yellow and the variant alanine is highlighted in green. (B) Principle of mosaic analysis of *Drosophila* histone mutants. Inductions of mosaic histone mutant clones begin with parental cells that are heterozygous for the histone locus. Mitotic crossover occurs at FRT40A with the supply of FLP. And upon appropriate segregation of sister chromatids (bottom box in the right part of the figure), homozygous *HisC* alleles either in WT or deleted forms can be generated. Because of their co-emergence, they are also referred to as twin clones. Homozygous *ΔHisC* clones are marked by the lack of GFP, while twin WT HisC clones show twice the GFP expression compared to the surrounding heterozygous cells. Since chromosome 3 is integrated with 12xHisGU, the endogenous source of H3 can be replaced by different H3 alleles in the *ΔHisC* clones. (*C*) and (*D*) Wing imaginal discs of homozygous *ΔHisC* clones supplemented with 12xHisGU transgenes carrying either H3 *WT*, *H3S28A* or *H3K27R* alleles. Immunostaining with the indicated antibodies is shown; DNA was stained with DAPI. Clones of interest are marked by the lack of GFP signal and are indicated by dashed lines. (*C*) Comparison of H3 staining in WT (GFP positive) tissue with clones containing *WT*, *H3S28A* or *H3K27R* histone replacement. Note that all histone replacement clones displayed normal H3 staining (red) level similar to the surrounding GFP positive (green) cells. (*D*) Comparison of H3K27me3 (red) levels in GFP-negative (histone replacement) clones with GFP-positive normal tissue. Note that *H3K27R* mutant cells (bottom row) were depleted of H3K27me3 despite having normal mitotic H3S28ph signal (green). *WT* clones supported robust H3K27me3 levels indistinguishable from the surrounding GFP positive cells. For clarity of composite micrographs, GFP is pseudocolored to blue in (*D*). Scale bars correspond to 10 µm.

Figure S2, related to Figure 2. Hox gene derepression profiles in histone mutants (*H3S28A* and *H3K27R*) clones and *Antp*^{Ns}.
(A) Micrographs showing full-scale imaginal discs described in Figure 2 and main text. For each imaginal disc, a selected region (dashed line) is magnified and displayed below the corresponding micrograph. Asterisks mark zones of endogenous expression of Scr and Ubx. Yellow arrowheads highlight weak Scr derepression occasionally detected in the notum region of wing discs in both *H3S28A* and *H3K27R* mutant clones. The white arrowhead indicates ectopic silencing of endogenous Ubx expression in the haltere disc carrying *H3K27R* clones. Scale bars of wing and eye-antenna discs represent 100 μm and those of leg discs represent 50 μm. (B) Antennal discs of *w*^{1118} (top panel) and *Antp*^{Ns} (bottom panel) were immunostained with the indicated antibodies. DNA was stained with DAPI. Arrowheads indicate ectopic expression of Antp and silencing of the antennal selector gene Hth. Scale bar corresponds to 100 μm.

Figure S3, related to Figure 3. Validation of clone induction of *dUtxΔ, H3S28A* double mutant and of in vivo RNAi against Aurora B kinase.
(A) Wing imaginal discs with clones homozygous of the combined *dUtxΔ, H3S28A* mutants were immunostained with the indicated antibodies. DNA was stained by DAPI. Clones were marked by the absence of GFP, which correspond to a drastic reduction of dUtx signal. (B) and (C) *Drosophila* wing imaginal discs of L3 larva with *nub-GAL4* directed RNAi against Aurora B at the wing pouch compartment marked by GFP and dotted lines. Wing discs were immunostained with the indicated antibodies and DNA was stained with DAPI. Scale bar of full-disc micrograph represents 100 μm and those of magnified regions in (*A*) represents 40 μm.

Figure S4, related to Figure 2. Nuclear staining patterns of Ph remain unchanged in *H3S28A* mutant.
(A) Immunostaining of wing imaginal discs for Ph. *WT* (top row) and *H3S28A* (bottom row) clones are identified by the lack of GFP signal and are marked by dashed lines. Samples were stained with DAPI and the indicated antibodies. Regions at the clone borders were further cropped and magnified. (B) Selections of mitotic cells from *WT* and *H3S28A* clones in wing imaginal discs were compiled to show the distribution of Ph during mitosis in the corresponding backgrounds. Only GFP-positive internal controls of *WT* clones are shown. Scale bars in (A) and (B) represent 10 μm and 2.5 μm, respectively.

Supplemental Experimental Procedures

***Drosophila* Stocks**

The following fly lines were used in this study

y, w; P{Ubi-GFP.D}33, P{Ubi-GFP.D}38, FRT40A (Bloomington #BL5189)

y, w, hsp70-flp; Df(2L) BSC104, FRT40A/CyO, twist-Gal4, UAS-GFP; MKRS/TM6B (Hodland Basler, 2012)

y, w; dUtxΔ, FRT40A/CyO, twist-Gal4, UAS-GFP (Copur and Muller, 2013)

y, w, hsp70-flp122; P{Ubi-GFP.D}33, P{Ubi-GFP.D}38, FRT40A; 6xHisGU

y, w, hsp70-flp122; P{Ubi-GFP.D}33, P{Ubi-GFP.D}38, FRT40A; $6xHisGU^{H3S28A}$

y, w, hsp70-flp122; P{Ubi-GFP.D}33, P{Ubi-GFP.D}38, FRT40A; $6xHisGU^{H3K27R}$

w; Df(2L) BSC104, FRT40A /CyO, Kr-Gal4, UAS-GFP; 6xHisGU

w; Df(2L) BSC104, FRT40A /CyO, Kr-Gal4, UAS-GFP; $6xHisGU^{H3S28A}$

w; Df(2L) BSC104, FRT40A /CyO, Kr-Gal4, UAS-GFP; $6xHisGU^{H3K27R}$

w; dUtxΔ, Df(2L) BSC104, FRT40A /CyO, Kr-Gal4, UAS-GFP; 6xHisGU

w; dUtxΔ, Df(2L) BSC104, FRT40A /CyO, Kr-Gal4, UAS-GFP; $6xHisGU^{H3S28A}$

y, w, ey-FLP1; P{Ubi-GFP.D}33, P{Ubi-GFP.D}38, FRT40A; 6xHisGU

y, w, ey-FLP1; P{Ubi-GFP.D}33, P{Ubi-GFP.D}38, FRT40A; $6xHisGU^{H3S28A}$

y, w ey-FLP1; P{Ubi-GFP.D}33, P{Ubi-GFP.D}38, FRT40A; $6xHisGU^{H3K27R}$

$Antp^{Ns}$*/TM3, Ser (Kindly provided by Walter Gehring lab.)*

w^{1118}

Mosaic analysis and Immunostaining

Primary antibodies used for immunostaining in this study:Hox antibodies were purchased from the Developmental Studies Hybridoma Bank (DSHB). Mouse anti-Scr (DSHB 6H4.1, 1:20), mouse anti-Antp (DSHB 8C11, 1:20), mouse anti-Ubx (DSHB FP3.38, 1:20), mouse anti-Abd-B (DSHB 1A2E9, 1:10), mouse anti-En (DSHB 4D9, 1:20), mouse anti-H3 (ActiveMotif 39763, 1:500), mouse antiH3S10ph (Millipore 05-806, 1:1000), rat anti-H3S28ph (Millipore MABE76, 1:1000), rabbit anti-H3K27me3 (Millipore 07-449, 1:500), rabbit anti-H3K27me2 (Upstate 07-452, 1:500), rabbit anti-H3K27me1 (Millipore 07-448, 1: 250), rabbit anti-H3K27ac (Abcam Ab4729, 1:500), rabbit anti-H34me3 (Millipore 04-745, 1:500), rabbit anti-Pc ((Grimaud et al., 2006), 1:500), goat anti-Ph ((Grimaud et al., 2006), 1:500), guinea pig anti-Hth (a gift from Ginés Morata, 1:200), rabbit anti- Aurora B (a gift from David Glover, 1: 200), rabbit anti-dUtx (a gift from Feng Tie and Peter J. Harte, 1: 200) chicken anti-GFP (Invitrogen A10262, 1:500).

Supplemental References

Copur, O., and Muller, J. (2013). The histone H3-K27 demethylase Utx regulates HOX gene expression in Drosophila in a temporally restricted manner. Development *140*, 3478-3485.

Grimaud, C., Bantignies, F., Pal-Bhadra, M., Ghana, P., Bhadra, U., and Cavalli, G. (2006). RNAi components are required for nuclear clustering of Polycomb group response elements. Cell *124*, 957-971.

Hodl, M., and Basler, K. (2012). Transcription in the absence of histone H3.2 and H3K4 methylation. Curr Biol *22*, 2253-2257.